Catalysis Today 153 (2010) 90–94

Contents lists available at ScienceDirect

Catalysis Today

journal homepage: www.elsevier.com/locate/cattod

# Density functional theory calculation on the promotion effect of $H_2$ in the selective catalytic reduction of $NO_x$ over Ag–MFI zeolite

Kyoichi Sawabe*, Taisuke Hiro, Ken-ichi Shimizu, Atsushi Satsuma

*Department of Molecular Design and Engineering, Graduate School of Engineering, Nagoya University, Furo-cho, Chikusa-ku, Nagoya 464-8603, Japan*

ARTICLE INFO

*Article history:*
Available online 2 June 2010

*Keywords:*
HC-SCR
Ag
MFI
DFT
TD-DFT

ABSTRACT

Density functional theory (DFT) calculation was used to study the hydrogen promotion effect for the selective catalytic reduction (HC-SCR) of $NO_x$ over Ag–MFI zeolite. The nature of the bond between an Ag atom and MFI is ionic. One of the roles of hydrogen addition is to neutralize the cationic Ag atom by forming an AgH molecule. We propose that the formation of a $Ag_4$ cluster is achieved by the AgH diffusion as follows: $2AgH + Ag\text{-}Z\text{-}Ag \rightarrow HAg_4H\text{-}Z \rightarrow Ag_4\text{-}Z + H_2$. With the presence of oxygen, the $HAg_4H$ cluster prefers the formation of $HOO^-$ adsorbate to the desorption of $H_2$. $O_2$ is physisorbed on the $Ag_4$ cluster. Thus, the $HAg_4H$ cluster is important for the activation of oxygen. Another role of hydrogen addition is to reproduce the $HAg_4H$ cluster from the $Ag_4$ cluster which is generated by the SCR reaction from $HOOAg_4H$ species. Since time dependent DFT (TD-DFT) calculation shows that the UV absorption bands of the $HAg_4H$ cluster are weak, UV–vis measurements are not adequate for the study of the reaction mechanisms of HC-SCR.



## 1. Introduction

The selective catalytic reduction of NO to $N_2$ by hydrocarbons (HC-SCR) in the presence of excess oxygen is a promising technique for removing $NO_x$ from lean-burn and diesel exhausts [1–4]. Since Satokawa [5] discovered that the addition of small amounts of hydrogen to the feed of the HC-SCR dramatically improved the performance of Ag-$Al_2O_3$ catalysts, several authors have investigated this "hydrogen effect" using different catalyst formulations and different gas mixes [6–24]. Several IR studies [12–17] showed that the addition of hydrogen resulted in the formation of the oxidized nitrogen- and carbon-containing species on the catalyst surface during the HC-SCR reaction. Shibata et al. [12] claimed that the rate of $NO_x$ reduction in the SCR reaction with $C_3H_8$ was directly dependent on the rate of partial oxidation of the hydrocarbon to surface acetate and that the essential role of $H_2$ was in the activation of molecular oxygen involved in the oxidation of hydrocarbons. Sazama et al. [25] reported that the addition of hydrogen peroxide also enhanced selective reduction of $NO_x$ with hydrocarbons. The addition of hydrogen promoted the formation of $Ag_4^{2+}$ cluster over Ag–MFI [7,8] and $Ag_n^{\delta+}$ cluster [22] over Ag-$Al_2O_3$. Shimizu et al. [22] reported that $O_2$ reduction with $Ag_n^{\delta+}$ yielded $O_2^-$ species. Therefore, Ag clusters formed by the addition of hydrogen may be related with the activation of oxygen. On the other hand, there are several reports against the idea that the cluster is active species. In the time dependent UV– vis experiment [15,22], the $NO_x$ conversion increased very rapidly upon the addition of $H_2$ whereas the band attributable to $Ag_n^{\delta+}$ clusters slowly increased. This indicated that the $Ag_n^{\delta+}$ clusters were not always related with high $NO_x$ conversion. Furthermore, Wichterlová et al. [16] showed that the addition of CO promoted the formation of Ag clusters but did not enhance the rate of the SCR reaction. Thus, the hydrogen promotion effect is still on the debate.

In this work, we have studied the hydrogen promotion effect for the selective catalytic reduction of $NO_x$ over Ag–MFI zeolite using the density functional theory (DFT) calculation. Heterolytic dissociation of hydrogen on the Ag–MFI is examined. The geometry optimization of sliver clusters shows that $Ag_4$ and $HAg_4H$ clusters are formed on two Al-substituted sites. In the simulation of UV spectra using the time dependent DFT calculation, the strong three bands appear for the $Ag_4$–MFI system whereas the $HAg_4H$–MFI gives the weak bands. The geometry optimization of $O_2$ adsorption on the $Ag_4$–MFI results in the physisorption and the electronic states of oxygen is almost identical to that of the isolated molecule. On the other hand, $O_2$ adsorption on the $HAg_4H$–MFI adsorption produces $HOO^-$ species.

## 2. Computational details

Density functional theory was used for the calculation of energy and geometry optimization. We adopted the hybrid functional of B3PW91 [26] for the DFT calculation. The choice of the DFT

* Corresponding author. Tel.: +81 52 789 2610; fax: +81 52 789 2610.
*E-mail address:* sawabe@apchem.nagoya-u.ac.jp (K. Sawabe).

0920-5861/$ – see front matter © 2010 Elsevier B.V. All rights reserved.
doi:10.1016/j.cattod.2010.03.078

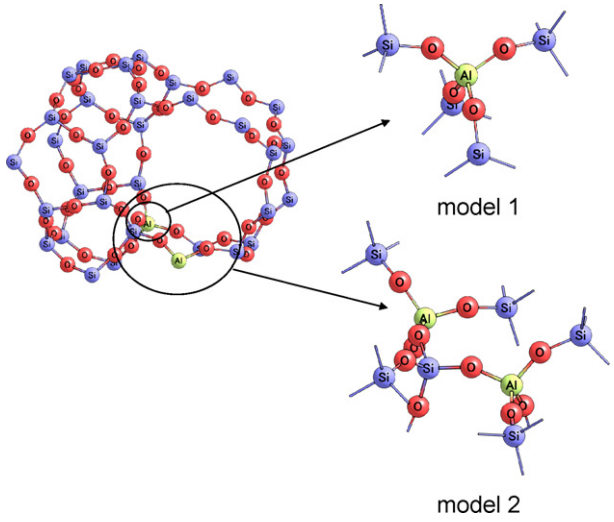


**Fig. 1.** Model clusters of MFI zeolite.

functional is critical for the calculation of Ag clusters. Although the B3LYP [27–29] is one of the popular hybrid functionals, this functional is not adequate for the calculation of metal clusters due to its failure to attain the homogeneous electron gas limit [30,31]. The basis sets used was SDD, which is the combination of Stuttgart–Dresden effective core potential (ECP) plus double zeta basis sets [32]. The time dependent DFT (TD-DFT) was used for the simulation of UV absorption spectra. Atomic charges and bond orders were investigated using the natural bond orbital (NBO) analysis [33]. All calculations were carried out with the Gaussian 03 program [34].

The restricted cluster models were widely used to study realistic zeolites [35–46]. In this study, we have adopted two cluster models shown in Fig. 1. In these models, Al atoms are assumed to occupy the T11 and T12 site [39,47]. The position of Al, Si and O atoms are fixed to those of the crystallographic structure in a MFI zeolite [48]. All dangling bonds are capped with hydrogen atoms. Partial optimization was adopted in this study; all atoms in the model clusters were fixed to the bulk position during the geometry optimization.

## 3. Results and discussion

### 3.1. Ag on MFI

#### 3.1.1. Interaction between Ag and MFI

Fig. 2a shows the optimized structure of a silver atom adsorbed on the model 1 cluster. The Ag adsorption has two-fold coordination to oxygen atoms and the bond lengths between Ag and O are

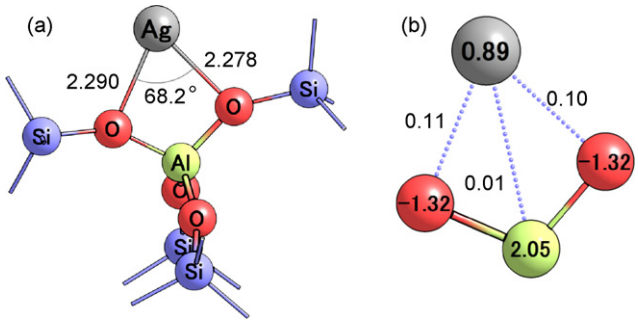


**Fig. 2.** (a) Bond lengths and an angle of the optimized structure of Ag adsorption on the model 1 cluster. The unit of the length is Å (b) natural charges of Ag, O and Al atoms and the bond orders between these atoms.

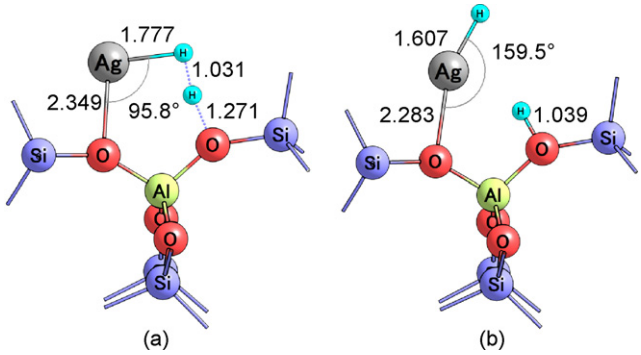


**Fig. 3.** Optimized structures of (a) the transition structure and (b) the product for $H_2$ dissociation on the Ag–MFI.

almost the same. The Ag— O coordination number in the Ag–MFI was reported to be 2.5 ± 0.5 [49], which cannot determine whether the Ag— O bindings are two-fold or three-fold coordination. We also carried out the geometry optimization starting from the initial structure having three-fold coordination of sliver and the resultant structure was less stable by 16.2 kcal/mol than that of Fig. 2a. Therefore, Ag atoms favor two-fold coordination to oxygen atoms of the $AlO_4$ tetrahedron. The average bond length between Ag and O is 2.28 Å, which is in good agreement with the experimental value of 2.30 Å [49] and the theoretical value of 2.34 Å by the combined quantum mechanics/interaction potential function [40]. This suggests that even a small cluster like the model 1 reproduce the local structure of Ag atoms or Ag clusters on the MFI.

Fig. 2b shows the natural charge of Ag and atoms of the adsorption site and the bond orders between them. The charge of Ag is 0.9 and the bond orders between Ag and its neighboring oxygen atoms are 0.1. Total charge of the model system is set to neutral. Thus, the transfer of an electron from the silver to the Al-substituted site makes the binding feature of Ag almost ionic.

#### 3.1.2. $H_2$ dissociation on Ag–MFI

We have calculated hydrogen dissociation on the Ag–MFI system. Fig. 3 shows the optimized structure of the transition structure and the structure of coadsorption of AgH and H as a product. Natural charges are summarized in Table 1. The transition structure was confirmed by an imaginary frequency which indicated the direction of $H_2$ dissociation path. Although the bond length between hydrogen atoms is elongated by 0.29 Å at the transition structure, the activation energy for the dissociation is as low as 10.7 kcal/mol. This is because the polarization of the hydrogen molecule takes place at the transition structure. The Ag— O site of the MFI serves as the Lewis acid–base pair and lowers the activation of the dissociation. The sum of charges of AgH in the product is 0.04. Therefore, the neutral AgH molecule is formed by the hydrogen dissociation on the Ag–MFI system.

In order to produce the Ag cluster, silver atoms must diffuse on the zeolite surface. Since the bonding nature between Ag and MFI is ionic, the neutralization of Ag must be necessary. Otherwise ionic species will be trapped during the diffusion because of the polarized character of the zeolite surface. There are two possible processes of the neutralization of the adsorbed Ag. One is the direct process via the electron transfer from zeolite to silver. Another is

**Table 1**
Natural charges of the transition structure and the product of AgH formation. H(-Ag) and H(-O) means hydrogen connected to Ag and oxygen, respectively.

| | Ag | H(-Ag) | H(-O) | O(-Ag) | O(-H) | Al |
|---|---|---|---|---|---|---|
| TS | 0.685 | −0.295 | 0.295 | −1.314 | −1.209 | 2.100 |
| Product | 0.262 | −0.222 | 0.493 | −1.299 | −1.141 | 2.094 |

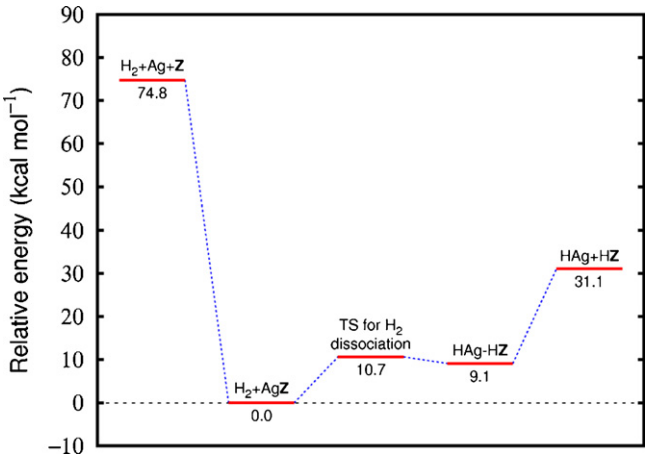


**Fig. 4.** Energy diagram of the Ag desorption from Ag–MFI and the AgH desorption via $H_2$ dissociation on the Ag–MFI. In this figure, the label "Z" means the model cluster of MFI.

the indirect process via the formation of AgH. In Fig. 4, we show the potential energy diagram for both the extraction of Ag and AgH from the isolated $H_2$ and Ag-Z system (Z means the model cluster). The extraction of the adsorbed Ag as a neutral atom requires 75 kcal/mol. The adsorbed AgH which has the relative energy of 9 kcal/mol is formed with the activation barrier of 11 kcal/mol, followed by the extraction of AgH with the endothermic energy of 22 kcal/mol. After all, the extraction of AgH requires 31 kcal/mol which is less than half of the energy of the neutral Ag extraction. Therefore, the AgH formation is favored for the neutralization of the adsorbed Ag atom. This result is consistent with the NMR [50] and IR [23] experiments, in which the addition of $H_2$ to the Ag–zeolite system showed the formation of the silver clusters and the OH bond. Thus, we proposed that the addition of $H_2$ promotes the diffusion of $Ag^+$ on MFI by the formation of AgH.

EXAFS studies [8,23] suggested that the $Ag_4$ cluster on the Ag–MFI system formed a tetrahedron. Before going to the calculation of the $Ag_4$–MFI system, we explain the bonding nature of the tetrahedral structure of the isolated $Ag_4$ cluster since the ionic nature of the Ag–MFI bond enables us the qualitative analysis of the structure using the isolated cluster. We have calculated the optimized structure of isolated $Ag_4$, $Ag_4^+$ and $Ag_4^{2+}$ clusters and found that the tetrahedral structure was only obtained for the $Ag_4^{2+}$ cluster. This is easily explained by the HOMO and LUMO picture. HOMO and LUMO of the silver cluster are mainly composed of 5s orbitals. HOMO of the $Ag_4^{2+}$ having a $T_d$ symmetry is an $a_1$ orbital which has no node between Ag atoms. The LUMOs are three degenerated $t_2$ orbitals which have a node between Ag atoms. The net charge less than 2+ means the electron occupation in the LUMO, which leads to the decrease of the bond between Ag atoms and the deformation from the tetrahedral structure. Thus, the orbital analysis suggests that the formation of the tetrahedral structure requires two electrons transfer from the $Ag_4$ cluster to the zeolite, which will take place on two Al-substituted sites. For this reason, we adopted the model 2 in Fig. 1 for the formation of the Ag cluster on the MFI.

### 3.2. $Ag_4$ and $H_2Ag_4$ cluster on MFI

#### 3.2.1. Formation of $Ag_4$ and $HAg_4H$ clusters

We have carried out the geometry optimization of the $Ag_4$ cluster on the model 2. The optimized result is shown in Fig. 5a. The bond lengths between silver atoms are in the range from 2.718 to 2.915 Å and the structure is a tetrahedron. The average bond length of Ag atoms is 2.79 Å which is in good agreement with the experimental value of 2.74 Å [23]. Natural charges of silver atoms are

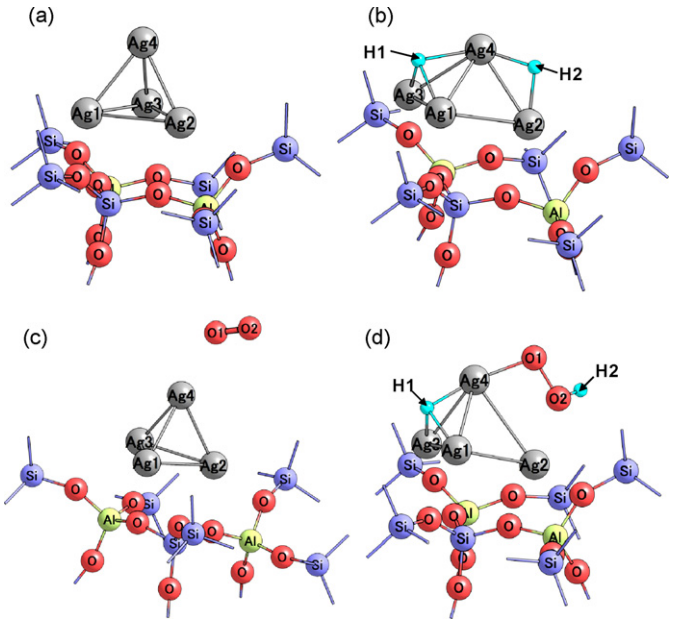


**Fig. 5.** Optimized structures of the adsorbed molecules on the model 2. (a) $Ag_4$-Z; (b) $HAg_4H$-Z; (c) $O_2Ag_4$-Z; (d) $HOOAg_4H$-Z.

shown in Table 2. Total sum of the charges of four Ag atoms is 1.72, but the charge distribution is not uniform. Three Ag atoms in the base are cationic and a silver atom at the vertex is almost neutral. This indicates that the Ag cluster has the potential to allow a slight electron transfer without breaking its form.

As mentioned before, silver diffuses as the AgH species. In order to examine that a $HAg_4H$-Z cluster is formed by the attack of two AgH species on two Ag atoms at the T11 and T12 sites, we have carried out the geometry optimization starting from the initial structure of two AgH fragments located around two Ag atoms on the T11 and T12 sites. The optimization results in the formation of the $HAg_4H$ cluster adsorption on the model 2 (Fig. 5b). As listed in Table 2, two hydrogen adsorbates are anionic and the net charge of the Ag cluster is 1.9. Therefore, this cluster is considered to be $H^-Ag_4^{2+}H^-$. The energy of the $HAg_4H$-Z cluster relative to that of the isolated $H_2$+$Ag_4$-Z system is high by 8 kcal/mol. Thus, the $HAg_4H$-Z structure is the intermediate for the formation of the $Ag_4$ cluster. We propose the reaction scheme of the $Ag_4$ cluster produced by the addition of hydrogen as follows:

$$4\text{Ag-Z} + 2\text{H}_2 \rightarrow 2\text{AgH} + 2\text{H-Z} + 2\text{Ag-Z} \rightarrow \text{HAg}_4\text{H-Z} + 2\text{H-Z} \rightarrow \text{Ag}_4\text{-Z} + \text{H}_2 + 2\text{H-Z}.$$

Totally one hydrogen molecule is consumed by the cluster formation. This is also consistent with the stoichiometry proposed by the experiment [23,24].

#### 3.2.2. UV absorption of $Ag_4$ and $HAg_4H$ clusters

TD-DFT calculation was carried out to simulate the UV absorption spectra of $Ag_4$–MFI and $HAg_4H$–MFI. We have examined the excitation energies in the range of 270 and 600 nm. The model 2 cluster alone has weak bands which have the oscillator strength ($f$)

**Table 2**
Natural charges of the adsorbed molecules. Refer to Fig. 5 for the position of atoms with number.

| | Ag1 | Ag2 | Ag3 | Ag4 | H1 | H2 | O1 | O2 |
|---|---|---|---|---|---|---|---|---|
| $Ag_4$-Z | 0.474 | 0.641 | 0.527 | 0.080 | | | | |
| $HAg_4H$-Z | 0.500 | 0.533 | 0.531 | 0.367 | −0.262 | −0.249 | | |
| $O_2Ag_4$-Z | 0.484 | 0.439 | 0.398 | 0.146 | | | −0.060 | 0.074 |
| $HOOAg_4H$-Z | 0.672 | 0.817 | 0.696 | 0.599 | −0.375 | 0.520 | −0.591 | −0.640 |

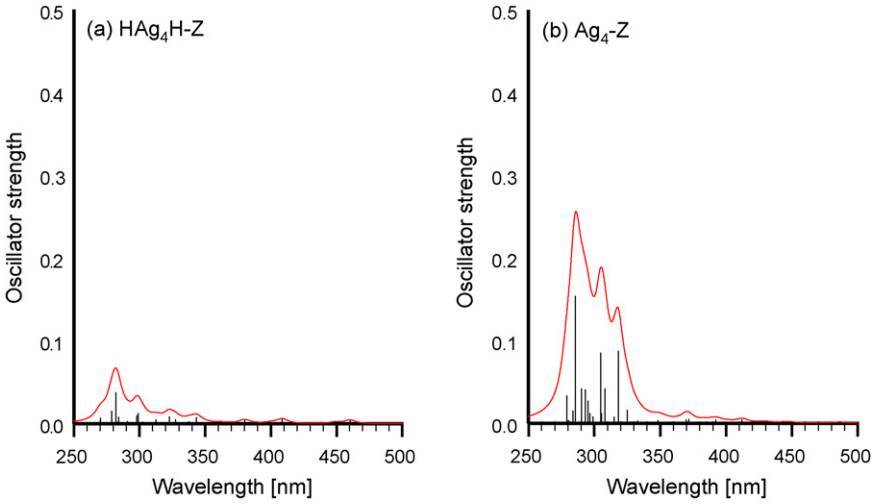


**Fig. 6.** Simulation of UV spectra of (a) $HAg_4H$-Z and (b) $Ag_4$-Z. Bars in the figures are the calculated values of TD-DFT. Red solid lines are simulated by overlapping Lorentz functions with the FWHM of 10 nm. (For interpretation of the references to colour in this figure legend, the reader is referred to the web version of the article.)

less than 0.01. Therefore, all strong absorption bands observed in this range involves the excitation of the electronic structure of the Ag cluster and/or the charge transfer between the cluster and the zeolite. Fig. 6 shows the simulation of UV spectra using the TD-DFT calculation. The $HAg_4H$-Z system has a weak absorption band at 282 ($f = 0.04$) nm. On the other hand, the $Ag_4$-Z system has three strong absorption bands at 286 ($f = 0.15$), 305 ($f = 0.09$) and 318 ($f = 0.09$) nm. The first strong band and the latter two bands correspond to the bands at 260 and 285 nm observed in the UV–vis spectra [7,8], respectively. These bands are attributed to the excitation among the electronic states of the $Ag_4$ cluster. As shown in Table 2, net charge of the $Ag_4$ cluster in the Ag-Z system is 1.72. If the $Ag_4^{2+}$ cluster is isolated from the zeolite, three absorption bands become a single band assigned to the HOMO-LUMO excitation of the cluster. In the $Ag_4$-Z system, the presence of the zeolite which splits the degenerated LUMO($t_2$) of $Ag_4^{2+}$ into three orbitals results in the appearance of three absorption bands. When hydrogen adsorbed on the $Ag_4$ cluster, partial occupation occurs in the unoccupied orbitals of the $Ag_4$ cluster. Thus, the absorption bands of the $HAg_4H$-Z system become weak. This result indicates that the UV–vis measurements are not adequate for the study of the reaction mechanisms in the case that the $HAg_4H$ cluster plays an important role in the HC-SCR reaction.

### 3.2.3. $O_2$ adsorption on $Ag_4$

Several experiments [15,22,24] suggested that the $O_2$ activation was required for the HC-SCR and superoxide ($O_2^-$) ions were observed in the ESR experiments [22,24]. In order to investigate whether the $Ag_4$ cluster activates the adsorbed oxygen, we have carried out the geometry optimization of the $O_2$ adsorption on the $Ag_4$-Z model. Since the isolated oxygen has the triplet state, both the singlet and the triplet states have been examined for the geometry optimization. Although no stable structure has been obtained in the singlet state, we have acquired the optimized structure in the triplet state (Fig. 5c). The bond distance of the adsorbed oxygen is 1.26 Å which is the same as that of the isolated oxygen. The bond order between oxygen atoms is 1.47 and the energy relative to that of the isolated system is −4 kcal/mol. Therefore, this structure is the physisorption of oxygen. Since the net charge of the adsorbed oxygen is almost neutral as listed in Table 2, the $Ag_4$ cluster cannot activate oxygen.

### 3.2.4. $O_2$ adsorption on $HAg_4H$

Although the $HAg_4H$ cluster is the intermediate for the formation of the $Ag_4$ cluster, the presence of $O_2$ may lead to the change in the reaction path to the $Ag_4$ cluster. We have examined several structures of the oxygen adsorption on the $HAg_4H$ cluster. As a result, we have obtained the optimized structure shown in Fig. 5d. The bond length between O1 and O2 is elongated to 1.52 Å. The bond orders of R(Ag4—O1), R(O1—O2), R(O2—H2) and R(O2—Ag2) are 0.34, 0.96, 0.74 and 0.09, respectively. The sum of charges of O1, O2 and H2 is −0.71. Therefore, the structure obtained indicates that the $HOO^-$ species is bound to the $HAg_4$ cluster with a single bond. This structure is the singlet ground state as same as hydrogen peroxide. Sazama et al. [25] reported that $H_2O_2$ enhances substantially selective reduction of $NO_x$ to nitrogen. Therefore, it is reasonable that the $HAg_4H$ cluster plays an important role for the SCR reaction by activating oxygen molecules.

Fig. 7 shows the energy diagram in which the starting point is set to the isolated system of $O_2$ and the $HAg_4H$ adsorbed structure. $O_2$ adsorption on the $Ag_4$ cluster following the desorption of $H_2$ takes place exothermically by 12 kcal/mol. On the other hand, the $O_2$ insertion into the H— Ag bond of the $HAg_4H$ adsorbate yields the relative energy of −32 kcal/mol. Although we did not calculate the transition state, we propose that the formation of the $HOO^-$ adsorbate is favored over the desorption of $H_2$. This hypothesis sup-

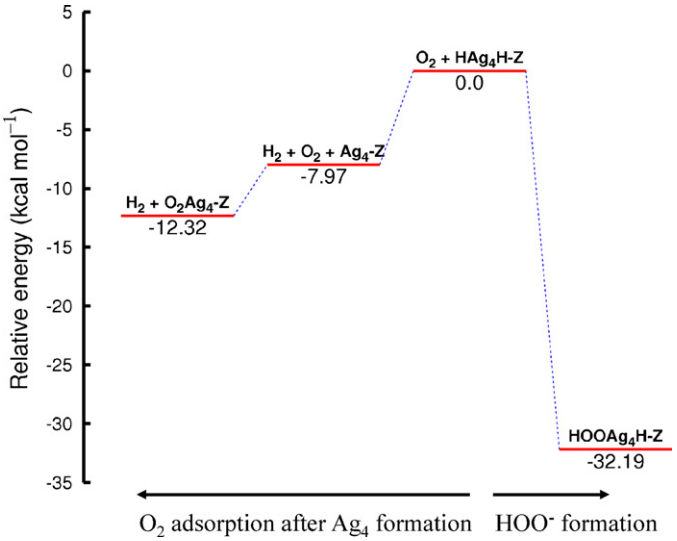


**Fig. 7.** Energy diagram of the $H_2$ desorption from $HAg_4H$-Z, followed by the $O_2$ adsorption on $Ag_4$-Z and the $O_2$ insertion into H— Ag bond of $HAg_4H$-Z.

ports the time dependence of NO conversion for the $C_3H_8$-SCR over $Ag/Al_2O_3$[22]. In this experiment, the addition of $H_2$ immediately increased NO conversion with the presence of $O_2$, whereas the UV bands attributed to the $Ag_4$ cluster appeared a short time after the introduction of $H_2$. This delay is explained by the immediate formation of the $HOOAg_4H$-Z since the UV bands of the $HAg_4H$-Z is weak. The UV bands attributed to the $Ag_4$ cluster appears when $H_2O_2$ is consumed from the $HOOAg_4H$ cluster in the SCR reaction. Furthermore, it is also explained that the SCR reaction was not enhanced by CO unlike $H_2$ in spite of the formation of Ag clusters promoted by the presence of CO [18,16]. This is because the $HAg_4H$ adsorbate is not reproduced without the presence of $H_2$.

## 4. Conclusions

Hydrogen addition has two effects on the HC-SCR reaction. One is the promotion of the formation of the $Ag_4$ cluster by generating the neutral AgH species, which can diffuse on the MFI surface. As a result, $HAg_4H$ cluster is formed by the following reaction: $2AgH + Ag\text{-}Z\text{-}Ag \rightarrow HAg_4H\text{-}Z$. $O_2$ insertion into the Ag-H bond of $HAg_4H$-Z leads to the formation of the active species of $HOO^-$ which is expected to be used in the partial oxidation of hydrocarbons for the HC-SCR reaction, whereas the $O_2$ adsorption on $Ag_4$ results in the physisorption. Thus, hydrogen is also necessary for the reproduction of the $HAg_4H$-Z from the $Ag_4$ cluster which is produced during the HC-SCR reaction,

The simulation of UV spectra for the $Ag_4$-Z and the $HAg_4H$-Z system explains the discrepancy in the several spectroscopic experiments which claimed the cluster formation is necessary or not for the HC-SCR reaction. Since the UV absorption bands of in the $HAg_4H$-Z system is weak, UV–vis experiments hardly detect the $HAg_4H$ cluster despite that this cluster plays important role in the HC-SCR reaction.

## Acknowledgment

This work was partly supported by a Grant-in-Aid for Scientific Research (KAKENHI) from the Ministry of Education, Science and Culture, Japan.

## References

[1] M. Iwamoto, H. Yahiro, Catal. Today 22 (1996) 5.
[2] H. Hamada, Catal. Today 22 (1996) 21.
[3] R. Burch, Catal. Rev. Sci. Eng. 46 (2004) 271.
[4] F. Klingstedt, K. Arve, K. Eränen, D.Y. Murzin, Acc. Chem. Res. 39 (2006) 273.
[5] S. Satokawa, Chem. Lett. 29 (2000) 294.
[6] S. Satokawa, J. Shibata, K. Shimizu, A. Satsuma, T. Hattori, Appl. Catal. B 42 (2003) 179.
[7] J. Shibata, Y. Takada, A. Shichi, S. Satokawa, A. Satsuma, T. Hattori, J. Catal. 222 (2004) 368.
[8] J. Shibata, K. Shimizu, Y. Takada, A. Shichi, H. Yoshida, S. Satokawa, A. Satsuma, T. Hattori, J. Catal. 227 (2004) 367.
[9] M. Richter, R. Fricke, R. Eckelt, Catal. Lett. 94 (2004) 115.
[10] M. Richter, U. Bentrup, R. Eckelt, M. Scneider, M.-M. Pohl, R. Fricke, Appl. Catal. B 51 (2004) 261.
[11] K. Eränen, F. Klingstedt, K. Arve, L.E. Lindfors, D. Murzin, J. Catal. 227 (2004) 328.
[12] J. Shibata, K. Shimizu, S. Satokaw, A. Satsuma, T. Hattori, Phys. Chem. Chem. Phys. 5 (2003) 2154.
[13] R. Burch, J.P. Breen, C.J. Hill, B. Krutzsch, B. Konrad, E. Jobson, L. Cider, K. Eränen, F. Klingstedt, L.E. Lindfors, Top. Catal. 30 (2004) 19.
[14] U. Bentrup, M. Richter, R. Fricke, Appl. Catal. B 55 (2005) 213.
[15] P. Sazama, L. Čapek, H. Drobná, Z. Sobalik, J.D. ědeček, K. Arve, B. Wichterlová, J. Catal. 232 (2005) 302.
[16] B. Wichterlová, P. Sazama, J. Breen, R. Burch, C. Hill, L. Čapek, Z. Sobalík, J. Catal. 235 (2005) 195.
[17] K. Shimizu, J. Shibata, A. Satsuma, J. Catal. 239 (2006) 402.
[18] J.P. Breen, R. Burch, C. Hardacre, C.J. Hill, J. Phys. Chem. B 109 (2005) 4805.
[19] R. Brosius, K. Arve, M. Groothaert, J. Martens, J. Catal. 231 (2005) 344.
[20] J. Breen, R. Burch, Top. Catal. 39 (2006) 53.
[21] K. Shimizu, A. Satsuma, Phys. Chem. Chem. Phys. 8 (2006) 2677.
[22] K. Shimizu, M. Tsuzuki, K. Kato, S. Yokota, K. Okumura, A. Satsuma, J. Phys. Chem. C 111 (2007) 950.
[23] K. Shimizu, K. Sugino, K. Kato, S. Yokota, K. Okumura, A. Satsuma, J. Phys. Chem. C 111 (2007) 1683.
[24] K. Shimizu, K. Sugino, K. Kato, S. Yokota, K. Okumura, A. Satsuma, J. Phys. Chem. C 111 (2007) 6481.
[25] P. Sazama, B. Wichterlová, Chem. Commun. (2005) 4810.
[26] A.D. Becke, J. Chem. Phys. 98 (1988) 5648.
[27] W.Y.C. Lee, R.G. Parr, Phys. Rev. B 37 (1988) 785.
[28] B. Miehlich, A. Savin, H. Stoll, H. Preuss, Chem. Phys. Lett. 157 (1989) 200.
[29] A.D. Becke, J. Chem. Phys. 98 (1993) 5648.
[30] J. Paier, M. Marsman, G. Kresse, J. Chem. Phys. 127 (2007) 24103.
[31] S. Zhao, Z.-H. Li, W.-N. Wang, Z.-P. Liu, K.-N. Fan, Y. Xie, H.F.S. Iii, J. Chem. Phys. 124 (2006) 184102.
[32] D. Andrae, U. Haussermann, H.S.M. Dolg, H. Preuss, Theor. Chim. Acta 77 (1990) 123.
[33] E.D. Glendening, A.E. Reed, J.E. Carpenter, F. Weinhold., NBO Version 3.1 as implemented in Gaussian 03.
[34] M. Frisch, Gaussian 03 (Revision C.02), Gaussian, Inc., Wallingford, CT, 2004.
[35] M.V. Frash, R.A. van Santen, Phys. Chem. Chem. Phys. 2 (2000) 1085.
[36] J. Limtrakul, P. Khongpracha, S. Jungsuttiwong, T.N. Truong, J. Mol. Catal. A: Chem. 153 (2000) 155.
[37] S. Jungsuttiwong, P. Khongpracha, T.N. Truong, J. Limtrakul, Stud. Surf. Sci. Catal. 135 (2001) 257.
[38] R.Z. Khaliullin, A.T. Bell, V.B. Kazansky, J. Phys. Chem. A 105 (2001) 10454.
[39] D. Nachtigallová, P. Nachtigall, J. Sauer, Phys. Chem. Chem. Phys. 3 (2001) 1552.
[40] M. Šilhan, D. Nachtigallovà, P. Nachtigallova, Phys. Chem. Chem. Phys. 3 (2001) 4791.
[41] S. Kasuriya, S. Namuangruk, P. Treesukol, M. Tirtowidjojo, J. Limtrakul, J. Catal. 219 (2003) 320.
[42] T. Atoguchi, S. Yao, J. Mol. Catal. A: Chem. 191 (2003) 281.
[43] E. Pidko, V. Kazansky, Phys. Chem. Chem. Phys. 7 (2005) 1939.
[44] A. Rattanasumrit, V. Ruangpornvisuti, J. Mol. Catal. A: Chem. 239 (2005) 68.
[45] C.O. Areán, M.R. Delgado, K. Frolich, R. Bulánek, A. Pulido, G.F. Bibiloni, P. Nachtigall, J. Phys. Chem. C 112 (2008) 4658.
[46] B. Ding, S. Huang, W. Wang, Appl. Surf. Sci. 254 (2008) 4944.
[47] M.H. Groothaert, K. Pierloot, A. Delabie, R.A. Schoonheydt, Phys. Chem. Chem. Phys. 5 (2003) 2135.
[48] H.V. Koningsveld, Acta Cryst. B43 (1987) 127.
[49] S. Bordiga, C. Lamberti, G.T. Palomino, F. Geobaldo, D. Arduino, A. Zecchina, Microporous Mesoporous Mater. 30 (1999) 129.
[50] T. Baba, N. Komatsu, H. Sawada, Y. Yamaguchi, T. Takahashi, H. Sugisawa, Y. Ono, Langmuir 15 (1999) 7894.